Engineering Notes

ENGINEERING NOTES are short manuscripts describing new developments or important results of a preliminary nature. These Notes cannot exceed 6 manuscript pages and 3 figures; a page of text may be substituted for a figure and vice versa. After informal review by the editors, they may be published within a few months of the date of receipt. Style requirements are the same as for regular contributions (see inside back cover).

Aircraft Wake Flow Effect and Horizontal Tail Buffet

Chintsun Hwang* and W.S. Pi†
Northrop Corporation, Hawthorne, Calif.

Introduction

DURING the transonic maneuver of a fighter aircraft, as the angle of attack increases, flow separation develops on the wing surfaces. The separated flow forms a high turbulence wake which engulfs the rear fuselage and tail surfaces, affecting the control performance of the aircraft. Furthermore, depending on the horizontal tail surface setting, leading edge or shock-induced separated flow may develop on the tail surfaces, which raises the local turbulence to an even higher level.

As part of a program to investigate the fluctuating pressure distribution and response behavior of a fighter aircraft in transonic maneuver, an F-5A scale model was tested in the NASA Ames Research Center's 11-ft transonic wind tunnel.[1,2] The model, with a number of static and dynamic pressure transducers imbedded in the lifting surfaces, was tested at various α's up to 16 deg. Test results of special interest to wake flow and horizontal tail buffet are described in this note.

Figure 1 depicts the aircraft wake-flow development at $\alpha = 14$ deg for two configurations featuring varying horizontal tail surface settings (δ_h). For $\delta_h = 0$, flow separation appears on the upper surfaces of the wing and the horizontal tail. As a result, high rms pressure level is expected on the tail upper surface. For $\delta_h = -10$ deg, and considering the wing downwash effect, the local angle of attack of the tail surface is less than that for $\delta_h = 0$ deg. As a result, no local flow separation takes place on the tail. The local rms pressure is thus caused essentially by the wake flow of the wing. As will be described later in the note, evidence of wing-tail flow interaction has been observed.

Test Data Presentation

Processing of the wake-flow and horizontal tail surface pressure data was performed with special attention to the establishment of an overall picture of the wake-flow pattern, as well as the effect of the horizontal tail surface setting under otherwise identical flow conditions. In Figs. 2 through 5, the dynamic pressure coefficients (rms) measured at transducers no. 14, 18, 22-25 are plotted vs the angle-of-attack α for $M = 0.925$ and $M = 0.75$. The configuration parameters appearing in these figures are δ_n/δ_f, the leading edge and trailing edge flap settings, and δ_h, the horizontal tail surface setting. In the plots, the solid lines denote the $\delta_h = 0$ deg cases and the dotted lines denote the $\delta_h = -10$ deg cases.

Received Aug. 30, 1978; revision received Oct. 26, 1978.

Index categories: Jets, Wakes, and Viscid-Inviscid Flow Interactions; Transonic Flow; Testing, Flight and Ground.

*Manager, Structural Dynamics Research. Associate Fellow AIAA.
†Engineering Specialist, Structural Dynamics Research.

The development of the wake-flow pattern, the effect of the tail surface settings, and the horizontal tail buffet phenomenon can be traced through the dynamic pressure coefficient development as functions of the angle-of-attack. For transducers no. 14 and 18, located on the wing upper surface, triangle marks are used to indicate the angle-of-attack setting α_s, above which $C_{\tilde{p}}$ values increased in such a manner as to indicate local flow separation. For $M = 0.925$, an examination of the $C_{\tilde{p}}$ data (Figs. 2a and 3a) showed that at times the deflection of the horizontal tail tended to delay or alternate the shock-induced flow separation in the portion of the wing directly upstream of the tail. The effect of the tail surface setting became less prominent as the angle of attack was increased to the 12-16 deg range.

In plots (b) of Figs. 2 through 5, for transducers no. 22 and 23 (tail upper surface), circles are used to indicate the transition point α_w (usually $> \alpha_s$) at which the rms dynamic pressures started to increase noticeably, usually reflecting the wake-flow effect of the wing. The wake-flow effect on the horizontal tail upper surface could be traced for both $\delta_h = 0$ and -10 deg cases. For configurations with $\delta_h = 0$ deg, the very high rms dynamic pressure of transducer no. 22 at high angles of attack indicated the horizontal tail top surface buffet. The extremely high $C_{\tilde{p}}$ value (0.298) at $\alpha = 16$ deg in Fig. 2b was one of the highest rms dynamic pressures recorded in the wind tunnel test program. The high dynamic pressure intensity on the tail surface for large α's is expected to affect the control characteristics of the aircraft, in addition to the direct excitation through the aircraft wing.

The flow patterns developed on the horizontal tail lower surface as shown in plots (c) of Figs. 2 through 5 were quite different from those on the upper surface. For the configurations with $\delta_h = 0$ deg, high rms dynamic pressures were observed at low angles of attack ($\alpha < 4$ deg) when the leading edge and trailing edge flaps of the model were deflected (solid lines in Figs. 2c and 4c). It can be visualized that the high dynamic pressures on the tail lower surface were caused by the wake flow with severe downwash effect due to the deflected flaps. For the configurations with $\delta_h = -10$ deg, the high $C_{\tilde{p}}$ values of transducers no. 24 and 25 at lower angle of attack settings [dotted lines in plots (c) of Figs. 2 through 5] indicated the shock-induced flow separation on the tail lower surface due to the negative tail deflection. As the angle of attack increased, the combined effects of tail buffet and wake flow due to wing buffet made the rms dynamic pressure levels of transducers no. 24 and 25 even higher (Figs. 2c and 4c), as

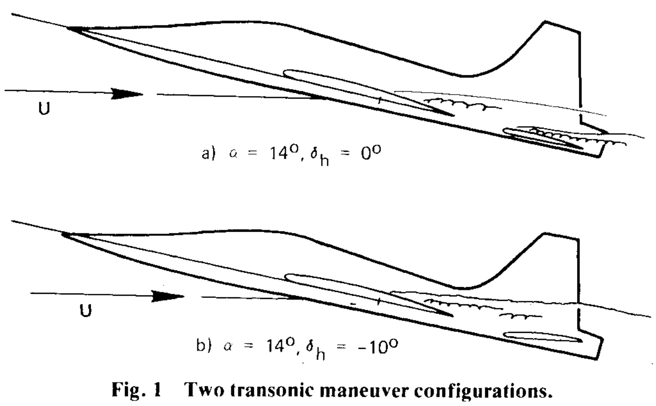

Fig. 1 Two transonic maneuver configurations.

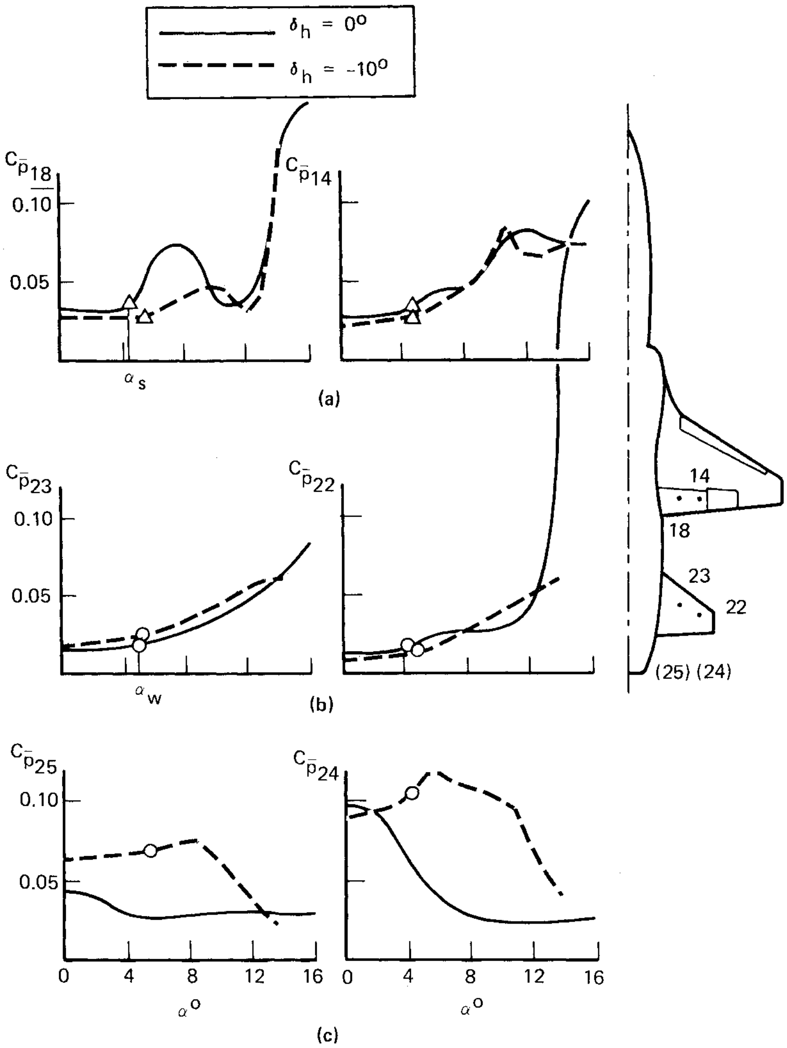

Fig. 2 Dynamic pressure coefficient comparison including tail deflection effect, $\delta_n/\delta_f = 5/12$ deg, $M = 0.925$, $Q_i = 18.2$ kN/m², $Re = 2.48 \times 10^6$. The pressure transducer locations are indicated. The numbers in parentheses (24,25) are for transducers on the tail's lower surface. All other numbers (14,18,22,23) are for transducers on the upper surfaces of the wing and the tail.

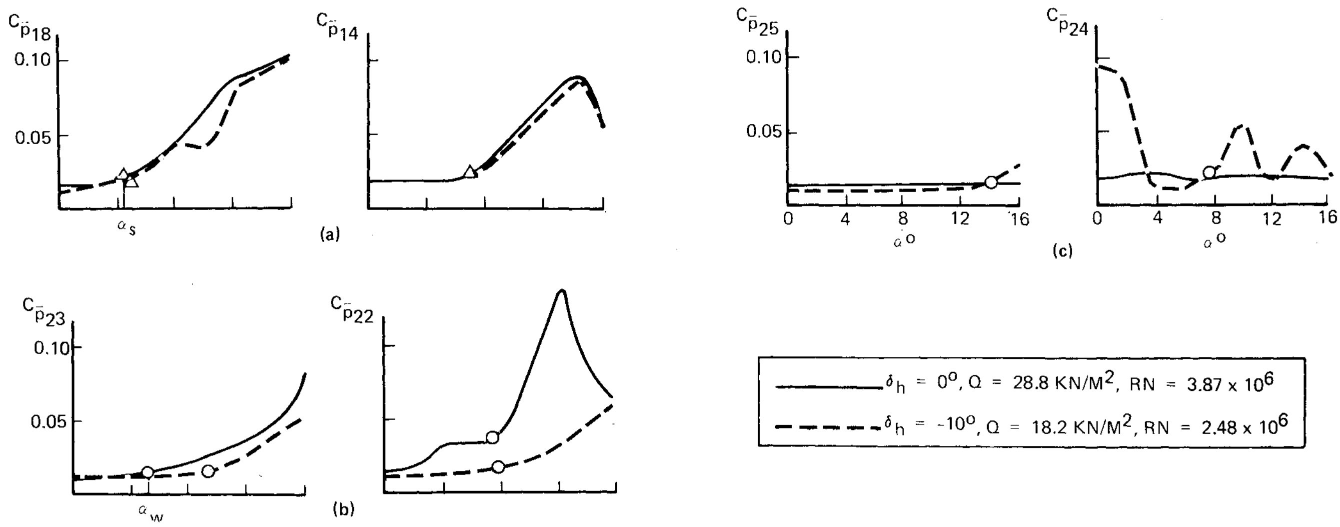

Fig. 3 Dynamic pressure coefficient comparison including tail deflection effect, $\delta_n/\delta_f = 0/0$ deg, $M = 0.925$.

compared to the cases with retracted leading and trailing edge flaps (Figs. 3c and 5c). However, the $C_{\bar{p}}$ values dropped when the angle of attack setting was further increased and the negative horizontal tail setting canceled the angle of attack effect. For the configurations with retracted leading edge and trailing edge flaps (Figs. 3c and 5c), the reduction in $C_{\bar{p}}$ for transducers no. 24 and 25 for $\delta_h = -10$ deg at very high $\alpha(>10$ deg) may be attributed to the fact that the wake effect of wing-flow separation was diminishing as far as the horizontal tail lower surface was concerned.

In conclusion, the dynamic pressure data on the tail surface at the specified flight conditions form the basis of the local dynamic loads determination. They also influence the control performance of the aircraft under maneuver conditions where

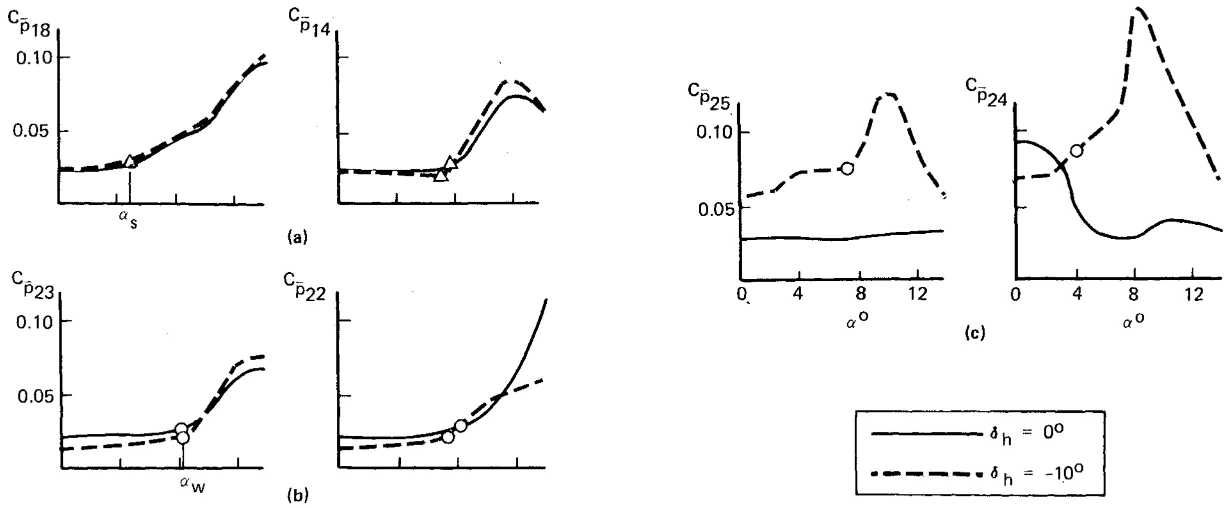

Fig. 4 Dynamic pressure coefficient comparison including tail deflection effect, $\delta_\psi/\delta_f = 5/12$ deg, $M = 0.75$, $Q = 15.6$ kN/m², $Re = 2.48 \times 10^6$.

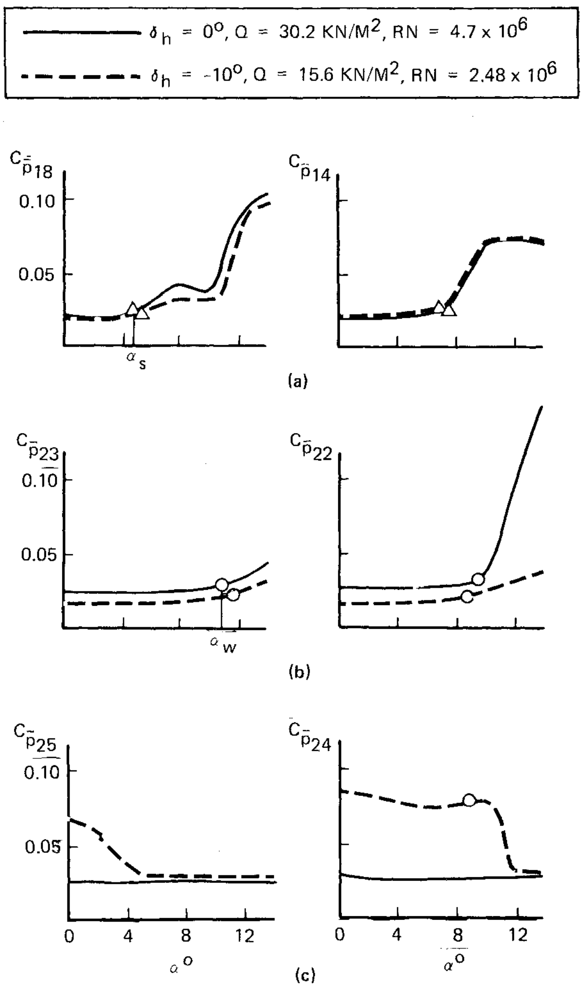

Fig. 5 Dynamic pressure coefficient comparison including tail deflection effect, $\delta_n/\delta_f = 0/0$ deg, $M = 0.75$.

buffet is encountered. The data presented in this note serve to demonstrate a number of contributing factors that affect the tail dynamic pressures in the transonic regime.

Acknowledgment

The test data reported in this note were acquired under NASA Ames Research Center Contract NAS2-8734, "F-5A Wind Tunnel Buffet Investigation." Mr. Charles Coe was the NASA program monitor.

References

[1]Hwang, C. and Pi, W.S., "Investigation of Steady and Fluctuating Pressures Associated with the Transonic Buffeting and Wing Rock of a One-Seventh Scale Model of the F-5A Aircraft," NASA Contract Rept., 3061, Nov. 1978.

[2]Hwang, C. and Pi, W.S., "Some Observations on the Mechanism of Aircraft Wing Rock," presented as Paper 78-1456 at the AIAA Aircraft Systems and Technology Meeting, Los Angeles, Calif., Aug. 21-23, 1978.

Transonic Shock-Boundary-Layer Interactions in Cryogenic Wind Tunnels

G.R. Inger*

Virginia Polytechnic Institute and State University, Blacksburg, Va.

Introduction

SINCE the transonic aerodynamics of missiles and aircraft can be significantly influenced by shock wave – boundary layer interaction effects, these effects should be adequately simulated in cryogenic high Reynolds number wind tunnel experiments. In addition to flight Mach and Reynolds numbers which are by design simulated in such facilities,[1] there are four other similitude parameters which may not be duplicated owing to the very low temperature-high pressure working fluid involved: wall to total temperature ratio T_w/T_t, specific heat ratio γ, viscosity temperature exponent ω, and Prandtl number Pr. The first is deemed especially important since in some proposed short duration cryogenic transonic wind tunnels the model is at a much higher temperature than

Presented as Paper 78-808 at the AIAA 10th Aerodynamic Testing Conference, San Diego, Calif., April 1978.

Index categories: Boundary Layers – Turbulent; Shock Waves; Transonic Flow.

*Professor, Dept. of Aerospace and Ocean Engineering. Associate Fellow AIAA.